Finite E β Jahn-Teller systems: a continued-fraction approach

Klaus G. Ziegler

Angaben zur Veröffentlichung / Publication details:

Ziegler, Klaus G. 2005. "Finite E β Jahn-Teller systems: a continued-fraction approach." *Physical Review B* 72 (7): 075120. https://doi.org/10.1103/physrevb.72.075120.

Finite $E\otimes\beta$ Jahn-Teller systems: A continued-fraction approach

K. Ziegler*
Institut für Physik, Universität Ausgburg, D-86135 Augsburg, Germany
(Received 25 February 2005; revised manuscript received 27 June 2005; published 16 August 2005)

A recursive method is developed to treat electrons coupled to phonons. It is applied to small systems with $E\otimes\beta$ Jahn-Teller coupling. Two cases are considered, a model with one electron and two orbitals on a single site (related to the Rabi Hamiltonian) and a model with two electrons on two sites. The corresponding Green's functions are represented by rational functions. It is found that the spectra change substantially when one phonon couples to the electron but are relatively robust under an increasing number of phonons.

DOI: 10.1103/PhysRevB.72.075120 PACS number(s): 71.27.+a, 31.30.Gs, 75.30.Et, 71.15.−m

I. INTRODUCTION

Small systems, like molecules or clusters of atoms, have attracted much attention in recent years because of new experimental techniques that provide detailed information of their spectral properties.[1–4] There are two mechanisms that control the physics of these small systems, one is the tunneling of electrons between different orbitals and different atoms, the other is the coupling between electrons and vibrational modes (phonons) of the molecules or clusters. For the latter the Jahn-Teller coupling scheme is relevant. Small Jahn-Teller systems can also be understood as building blocks for lattice Jahn-Teller systems which play a crucial role in solid-state physics, for instance, in the form of transition metal oxids.[5]

The main problem of treating electrons that couple to phonons is that even for small systems with one or a few electrons the Hilbert space is infinite dimensional. This implies a complex spectrum with level crossing and avoided level crossing.[6] There are various treatments of small Jahn-Teller systems, e.g., exact numerical diagonalization with truncated phonon spectrum,[7–9] Monte Carlo simulations,[10] or variational methods.[11] In this paper a systematic recursive procedure for treating the phonons in small electronic systems is developed and applied to several examples. It is based on a projection formalism.[12] The method is quite flexible, can easily deal with degeneracies, and was previously introduced to two-component bosons on a lattice.[13] The central idea is to approximate the elements of a Green's function systematically by standard (e.g., rational) functions.

The paper is organized as follows: In Sec. II the evolution of a quantum state and its connection to a projected Green's function is briefly discussed. The continued-fraction approach is developed in Sec. III. Then in Sec. IV two models with Jahn-Teller coupling are introduced, a single-site model where an electron tunnels between two orbitals and a model where two electrons tunnel between two sites. The application of the continued-fraction approach to these models is explained in Sec. V and the results are discussed in Sec. VI.

II. EVOLUTION OF STATES: PROJECTED DYNAMICS

The evolution of a quantum state $|\Psi_t\rangle$ during the time interval $[0,\tau]$ is given by

$$|\Psi_\tau\rangle = e^{iH\tau}|\Psi_0\rangle,$$

where the Hamiltonian H is measured in units of $\hbar$. A Laplace transformation for a positive time τ gives for $Imz<0$ a resolvent:

$$\int_0^\infty e^{-iz\tau}|\Psi_\tau\rangle d\tau = \int_0^\infty e^{-iz\tau}e^{iH\tau}d\tau|\Psi_0\rangle = i(z-H)^{-1}|\Psi_0\rangle. \tag{1}$$

Suppose that the initial state $|\Psi_0\rangle$ is from a restricted Hilbert space of low energy, the Green's function $(z-H)^{-1}$ acts on a restricted Hilbert space, represented by the projector P_0 and the projected resolvent $(z-H)^{-1}P_0$. To evaluate the probability for the system to return to the initial state $|\Psi_0\rangle$, the following quantity must be evaluated:

$$\langle\Psi_0|\Psi_\tau\rangle = (i/2\pi)\int_{-\infty}^\infty e^{iz\tau}\langle\Psi_0|(z-H)^{-1}|\Psi_0\rangle dz.$$

If E_j are the eigenvalues of H we can write for Eq. (1)

$$\langle\Psi_0|(z-H)^{-1}|\Psi_0\rangle = \sum_j \frac{|\langle E_j|\Psi_0\rangle|^2}{z-E_j}. \tag{2}$$

The poles of this expression are the characteristic frequencies of the evolution, starting from the projected Hilbert space and returning to it. The imaginary part of the Green's function gives the corresponding spectral density. In particular, the imaginary part of the projected resolvent in Eq. (2) reads

$$Im\langle\Psi_0|(E-i\epsilon-H)^{-1}|\Psi_0\rangle = \epsilon\sum_j \frac{|\langle E_j|\Psi_0\rangle|^2}{(E-E_j)^2+\epsilon^2}. \tag{3}$$

For small ϵ this results shows peaks of height $|\langle E_j|\Psi_0\rangle|^2/\epsilon$ at the eigenvalues E_j. Thus this height at $E=E_j$ is a direct measure of the overlap between the initial state $|\Psi_0\rangle$ and the eigenstate $|E_j\rangle$ for $\epsilon\sim 0$.

III. PROJECTION FORMALISM AND CONTINUED-FRACTION REPRESENTATION

After this preparation the goal is to evaluate the projected Green's function $P_0(z-H)^{-1}P_0$, where P_0 projects the states of the entire Hilbert space to the subspace $\mathcal{H}_0$. For a sym-

metric Hamiltonian H it satisfies the identity[13]

$$P_0(z-H)^{-1}P_0=[P_0(z-H)P_0-P_0HP_1(z-H)_1^{-1}P_1HP_0]_0^{-1}, \tag{4}$$

where $P_1=\mathbf{1}-P_0$ projects onto the Hilbert space $\mathcal{H}_1$ that is complementary to $\mathcal{H}_0$. The next calculational step is to treat the projected operators of the inverse on the right-hand side. First, there is the projection of P_0HP_0 which is completely restricted to $\mathcal{H}_0$. And second, there is P_1HP_0 and its transposed operator P_0HP_1 which connects the Hilbert spaces $\mathcal{H}_0$ and $\mathcal{H}_1$. Now it is assumed that the Hamiltonian H does not connect the entire Hilbert space $\mathcal{H}_1$ with $\mathcal{H}_0$ but only a subspace $\mathcal{H}_2$. This is a condition that is valid for typical Hamiltonians in physics. In other words, the Hamiltonian H satisfies the conditions

$$P_0HP_1=P_0HP_2, \quad P_1HP_0=P_2HP_0 \quad (P_2\neq P_1).$$

Thus H has defined a new projection $\mathcal{H}_2$ and Eq. (4) becomes

$$P_0(z-H)^{-1}P_0=[P_0(z-H)P_0-P_0HP_2(z-H)_1^{-1}P_2HP_0]_0^{-1}. \tag{5}$$

Now the identity used in Eq. (4) can be applied again to $P_2(z-H)_1^{-1}P_2$ on the right-hand side. A repetition of this procedure creates a hierarchy of projectors P_k onto Hilbert spaces $\mathcal{H}_k$. It is based on the fact that the projector P_{2j+1} is created from P_{2j-1} and P_{2j} as

$$\mathcal{H}_{2j+1}=\mathcal{H}_{2j-1}\setminus\mathcal{H}_{2j}\subset\mathcal{H}_{2j-1},$$

i.e., $\mathcal{H}_{2j+1}$ is the complement of $\mathcal{H}_{2j}$ on $\mathcal{H}_{2j-1}$. Moreover, the projector P_{2j+2} is created by the assumption that the Hamiltonian H satisfies the conditions

$$P_{2j+1}HP_{2j}=P_{2j+2}HP_{2j} \text{ and } P_{2j}HP_{2j+1}=P_{2j}HP_{2j+2}. \tag{6}$$

The hierarchy of projected Hilbert spaces is schematically shown in Fig. 1. It implies a recursion relation that connects pairs of projected Green's functions:

$$P_{2j}(z-H)_{2j-1}^{-1}P_{2j}=[P_{2j}(z-H)_{2j-1}P_{2j}-P_{2j}HP_{2j+2}\times(z-H)_{2j+1}^{-1}P_{2j+2}HP_{2j}]_{2j}^{-1}.$$

By using $G_{2j}=P_{2j}(z-H)_{2j-1}^{-1}P_{2j}$ and $H_{j,j+1}=P_{2j}HP_{2j+2}$ this reads

$$G_{2j}=[z-P_{2j}HP_{2j}-H_{j,j+1}G_{2j+2}H_{j+1,j}]_{2j}^{-1}. \tag{7}$$

Further simplifications are possible if it is assumed that the Hamiltonian H can be written as a sum of two Hamiltonians as $H=H_0+H_1$ with the following properties:

(1) H_0 must stay inside the projected Hilbert space: $H_0P_{2j}=P_{2j}H_0P_{2j}$ and $P_{2j}H_0=P_{2j}H_0P_{2j}$.

(2) H_1 maps from $\mathcal{H}_{2j}$ to $\mathcal{H}_{2j+2}$:

$$H_1:\mathcal{H}_{2j}\to\mathcal{H}_{2j+2},$$

where $\mathcal{H}_{2j}$ is orthogonal to $\mathcal{H}_{2j+2}$. Examples shall be discussed subsequently.

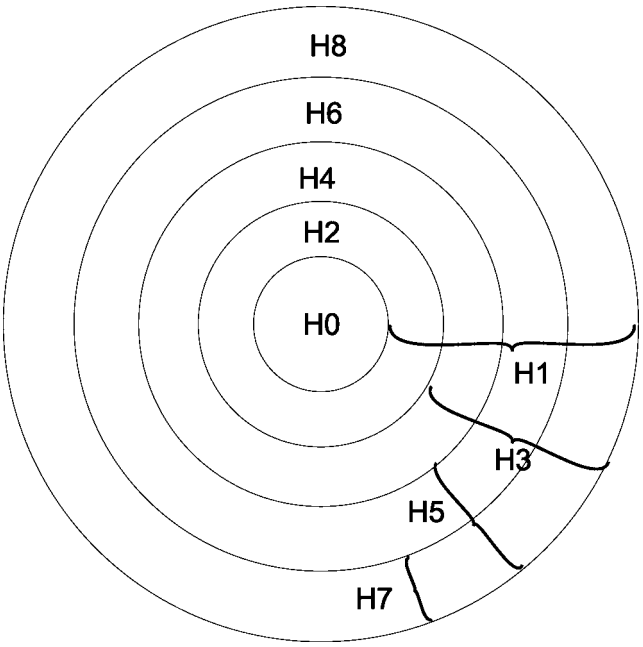

FIG. 1. Schematic hierarchy of recursively projected Hilbert spaces. The spaces $H0,H2,\ldots,H8$ are indicated by the rings and the brackets indicate the set of rings that belong to the corresponding space $H1,H3,\ldots,H7$. The initial projection is $H0$, the other projections $H2,H4,\ldots,H8$ are created by the Hamiltonian due to Eq. (6). $H1$ is the complement of $H0$ on the entire Hilbert space, $H3$ is the complement of $H2$ on $H1$, etc. The complement of $H8$ is empty such that $H8=H7$.

IV. MODELS: $E\otimes\beta$ JAHN-TELLER COUPLING

The Jahn-Teller electron-phonon coupling describes electrons that may occupy two possible orbitals. The latter can be understood formally as a pseudospin σ with values $\sigma=\uparrow,\downarrow$. On a molecule, a cluster or a lattice one phonon mode couples to electrons at each site, where the interaction energy is a sum over all sites $j=1,\ldots$:

$$H_{eph}=g\sum_j(b_j^\dagger+b_j)(n_{j\uparrow}-n_{j\downarrow}).$$

$n_{j\sigma}$ is the electronic number operator at site j and orbital σ, and $b_j^\dagger$ (b_j) is the creation (annihilation) operator of a phonon.

The simplest case considered in this paper is a single site with two orbitals, where an electron can tunnel between the two orbitals. This problem is also well-known in atomic physics under the name of Rabi Hamiltonian.[14] An extension is a two-site system with two orbitals per site and with two electrons. The model is simple if both electrons are in the same orbital because of Pauli blocking. Therefore, we consider the case where the two electrons sit in different orbitals. They can tunnel between the two sites and are coupled to each other via the electron-phonon interaction.

A. Single site: Jahn-Teller effect with interorbital tunneling

There are two electronic states, either the electron is in orbital $\uparrow$ or in orbital $\downarrow$. Moreover, there are N (N

$=0,1,\ldots$) phonons. Thus the Hilbert space is spanned by

$$|N,\uparrow\rangle, \quad |N,\downarrow\rangle.$$

For electronic tunneling rate t between the two orbitals the resulting Rabi Hamiltonian reads

$$H = t\sigma_1 + \omega_0\sigma_0 b^\dagger b + g\sigma_3(b^\dagger + b), \tag{8}$$

where the Pauli matrices refer to the electronic states for the two orbitals.

B. Two sites: Jahn-Teller effect with intersite tunneling

The extension of the model to two sites and two electrons provides the opportunity to study the effect of electron-electron interaction and electronic correlations. For a given pair of electrons, represented by integer numbers $n_{j\sigma}=0,1$, states with two electrons that occupy different orbitals are considered. (Electrons stay in their orbital because inter-orbital tunneling is not included.) Then the following electronic states are available:

$$|\downarrow,\uparrow\rangle, \quad |\uparrow,\downarrow\rangle, \quad |\downarrow\uparrow,0\rangle, \quad |0,\downarrow\uparrow\rangle. \tag{9}$$

The tunneling of the electrons and their Coulomb (Hubbard-type) interaction is defined by the Hamiltonian H_e and by the dispersionless phonons with energy ω_0 as

$$H_e = -t\sum_{\sigma=\uparrow,\downarrow}(c_{1\sigma}^\dagger c_{2\sigma} + c_{2\sigma}^\dagger c_{1\sigma}) + U\sum_{j=1,2} n_{j\uparrow}n_{j\downarrow}, \quad H_{ph} = \omega_0\sum_{j=1,2} b_j^\dagger b_j.$$

$c_j^\dagger$ (c_j) is the creation (annihilation) operator of an electron. The electronic spin is not taken into accout here, i.e., spin-polarized states are considered. The electron-phonon interaction reads

$$H_{eph} = g\sum_{j=1,2}(b_j^\dagger + b_j)(n_{j\uparrow} - n_{j\downarrow}),$$

leading to the total Hamiltonian $H=H_e+H_{ph}+H_{eph}$.

V. APPLICATION OF THE CONTINUED-FRACTION APPROACH TO SMALL SYSTEMS

If H_1 is a small perturbation to H_0 the resolvent of $H=H_0+H_1$ can be written as a Neumann series:

$$(z-H)^{-1} = (z-H_0-H_1)^{-1} = (z-H_0)^{-1}\sum_{l\geqslant 0}[H_1(z-H_0)^{-1}]^l.$$

Truncation after a finite number of terms yields poles only from the zeros of $z-H_0$. This is often insufficient to observe a realistic pole structure of the Green's function $(z-H)^{-1}$. The approximation can be improved by using a Padé approximation[15] or a partial summation of infinitely many contributions.[12] A systematic approach is the continued fraction of Sec. III that approximates the projected Green's function $P_0(z-H)^{-1}P_0$ by rational functions with a complex pole structure. Depending on the regime (weak or strong electron-phonon interaction) there are two different approximation schemes.

A. Strong electron-phonon interaction

If the tunneling energy is small in comparison with the electron-phonon interaction it is possible to separate the Hamiltonian as $H=H_0+H_1$ with

$$H_0 = \omega_0\sigma_0 b^\dagger b + g\sigma_3(b^\dagger + b), \quad H_1 = t\sigma_1 \tag{10}$$

and consider H_1 as a perturbation in the sense of the discussion in Sec. III. To diagonalize H_0, the Lang-Firsov transformation can be used as a unitary transformation

$$u = \begin{pmatrix} e^{\alpha(b^\dagger - b)} & 0 \\ 0 & e^{-\alpha(b^\dagger - b)} \end{pmatrix}, \quad \alpha = g/\omega_0$$

with

$$uH_0u^\dagger = H_0' = \omega_0(b^\dagger b - \alpha^2)\sigma_0.$$

The transformation of H_1 creates a complicated expression H_1' that connects states with different phonon numbers. This makes it difficult to perform the iteration of the recursion relation. For P_0 being the projection on the Hilbert space with $N=0$ phonons *after* the Lang-Firsov transformation was applied, Eq. (4) gives

$$P_0(z-H')^{-1}P_0 = [P_0(z-H_0')P_0 - P_0H_1'P_1 \times (z-H')_1^{-1}P_1H_1'P_0]_0^{-1},$$

and by using the approximation $(z-H')_1^{-1} \approx (z-H_0')_1^{-1}$ one obtains

$$P_0(z-H')^{-1}P_0 \approx [P_0(z-H_0')P_0 - P_0H_1'P_1 \times (z-H_0')_1^{-1}P_1H_1'P_0]_0^{-1}.$$

After a lengthy but straightforward calculation this becomes

$$= \left[z - \frac{t^2e^{-\alpha^2}}{\omega_0}\left(\frac{1}{(z/\omega_0+\alpha)} - \gamma^*(-z/\omega_0-\alpha^2,-4\alpha^2)\right)\right]^{-1}\sigma_0 \tag{11}$$

with the incomplete Gamma function[16]

$$\gamma^*(a,y) = \sum_{m\geqslant 0}\frac{1}{m!}\frac{(-y)^m}{a+m}.$$

The renormalization factor $e^{-\alpha^2/2}$ of the tunneling rate t is a well-known effect of the phonons, originally established in polaron physics,[7,8] and also observed in the strong-coupling regime of the Hubbard-Holstein model.[17] Results of the iteration are shown in Fig. 2 for the spectral density. It should be noticed that the expression for $P_0(z-H)^{-1}P_0$ with the projection P_0 *before* the Lang-Firsov transformation was applied is more complicated.

B. Weak electron-phonon interaction

If the tunneling energy is large in comparison with the electron-phonon interaction a different separation of the Hamiltonian $H=H_0+H_1$ is needed:

$$H_0 = t\sigma_1 + \omega_0 b^\dagger b\sigma_0, \quad H_1 = g\sigma_3(b^\dagger + b).$$

Equation (7) can be truncated for N phonons. This leads to the equations

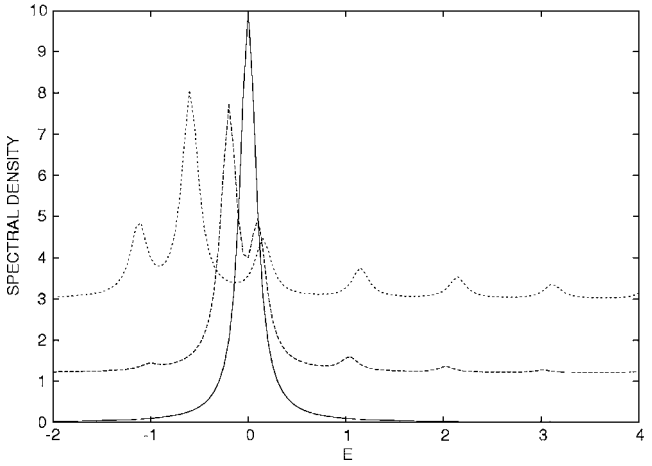

FIG. 2. Strong coupling approach: The spectral density of the single-site model $-Im(\langle\uparrow|(z-H)^{-1}|\uparrow\rangle$ for $z=E+0.05i$, $g=1$, $N=1$, and $t=0,0.5,1$, where all energies are measured in units of the phonon frequency ω_0. ($6t$ is added to the curves for better visibility.)

$$G_{2j}=[z\sigma_0-t\sigma_1-j\omega_0\sigma_0-g^2\sigma_3 bG_{2j+2}b^\dagger\sigma_3]^{-1}_{N-j}$$

with terminating condition

$$G_{2N}=((z-N\omega_0)\sigma_0-t\sigma_1)^{-1}=\frac{1}{(z-N\omega_0)^2-t^2}\begin{pmatrix}z-N\omega_0 & t\\ t & z-N\omega_0\end{pmatrix}.$$

Some results of the iteration for the spectral density are shown in Fig. 3.

The single-site model of Eq. (8) was also studied in the context of quantum optics[18] and in the context of the two-site Holstein model.[19] The continued-fraction method of these works is the same as the one discussed in Sec. V B, except for an additional diagonalization of the 2×2 matrix structure. Moreover, the continued fraction is obtained directly from the iteration of a tridiagonal matrix with scalar elements and does not require the projection of the Hilbert space.

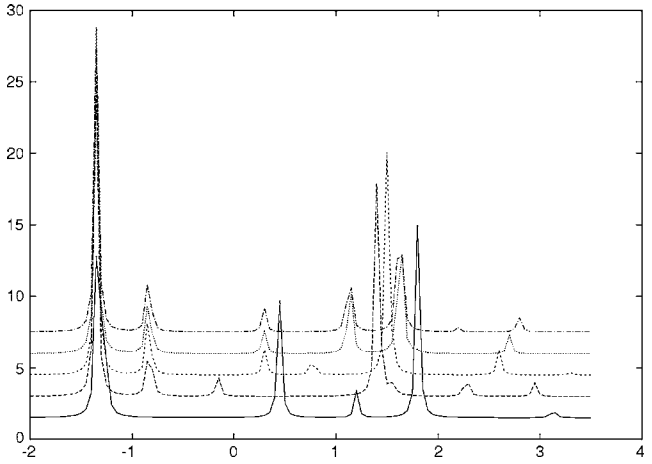

FIG. 3. The spectral density $-Im(\langle\uparrow|(z-H)^{-1}|\uparrow\rangle$ of the single-site model with $z=E+0.02i$, $t=g=1$ and $N=1,2,3,4,5$. ($1.5N$ is added to the curves for better visibility.)

C. Two sites with two electrons

The Hamiltonian of Sec. IV B reads in the basis of Eq. (9)

$$H_e=\begin{pmatrix}0&0&-t&-t\\0&0&t&t\\-t&t&U&0\\-t&t&0&U\end{pmatrix},\qquad H_{ph}=\omega_0(b_1^\dagger b_1+b_2^\dagger b_2)\begin{pmatrix}1&0&0&0\\0&1&0&0\\0&0&1&0\\0&0&0&1\end{pmatrix}, \tag{12}$$

and

$$H_{eph}=g\begin{pmatrix}-\Delta^\dagger-\Delta&0&0&0\\0&\Delta^\dagger+\Delta&0&0\\0&0&0&0\\0&0&0&0\end{pmatrix}\equiv g(\Delta^\dagger+\Delta)S, \tag{13}$$

where $\Delta=b_1-b_2$. Thus Δ ($\Delta^\dagger$) lowers (raises) the number of phonons by one.

Using $H_0=H_e+H_{ph}$ and $H_1=H_{eph}$ (this is the weak-coupling case) the recursion relation of Eq. (7) reads

$$G_j=[z-P_j(H_e+H_{ph})P_j-g^2P_j\Delta SG_{j+1}S\Delta^\dagger P_j]^{-1}_j \tag{14}$$

with the terminating condition for a maximum of N phonons:

$$G_N=[z-P_N(H_e+H_{ph})P_N]^{-1}_N. \tag{15}$$

This $4(N+1)\times 4(N+1)$ matrix is diagonal in terms of the phonon states. There are $N+1$ different phonon states, since there can be k $(=0,1\ldots,N)$ phonons at the first site and $N-k$ phonons at the second site.

The action of the phonon operators $P_j\Delta$ and $\Delta^\dagger P_j$ on the $4(j+2)\times 4(j+2)$ phonon-diagonal matrix G_{j+1} creates a $4(j+1)\times 4(j+1)$ phonon-diagonal matrix with 4×4 matrices $D(k,j+1-k)=G_{j+1}(k,j+1-k|k,j+1-k)$:

$$P_j\Delta\begin{pmatrix}D(0,j+1)&0&\ldots&0\\0&\ddots&\ddots&\vdots\\\vdots&\ddots&\ddots&0\\0&\ldots&0&D(j+1,0)\end{pmatrix}\Delta^\dagger P_j=2\begin{pmatrix}D(0,j)&0&\ldots&0\\0&\ddots&\ddots&\vdots\\\vdots&\ddots&\ddots&0\\0&\ldots&0&D(j,0)\end{pmatrix}.$$

This can be used to perform the iterations according to Eqs. (14) and (15). The results for the spectral density of the

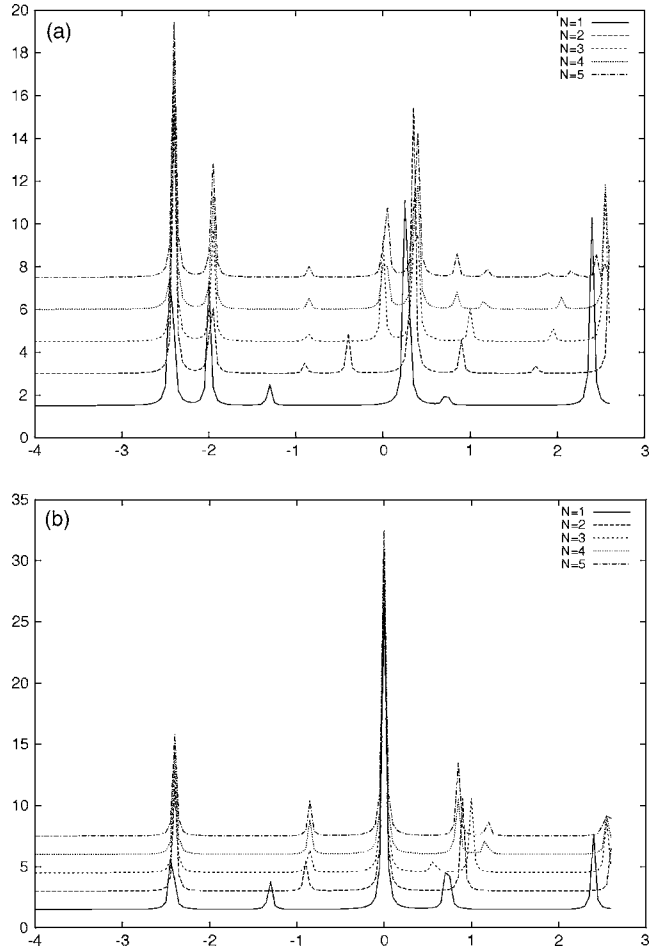

FIG. 4. The spectral densities of the two-site model with $z=E+0.02i$, $t=g=1$, $U=0$, and $N=1,2,3,4,5$: $-Im(\langle\downarrow,\uparrow|(z-H)^{-1}|\downarrow,\uparrow\rangle$ (upper panel) and $-Im(\langle\downarrow\uparrow,0|(z-H)^{-1}|\downarrow\uparrow,0\rangle$ (lower panel). ($1.5N$ is added to the curves for better visibility.)

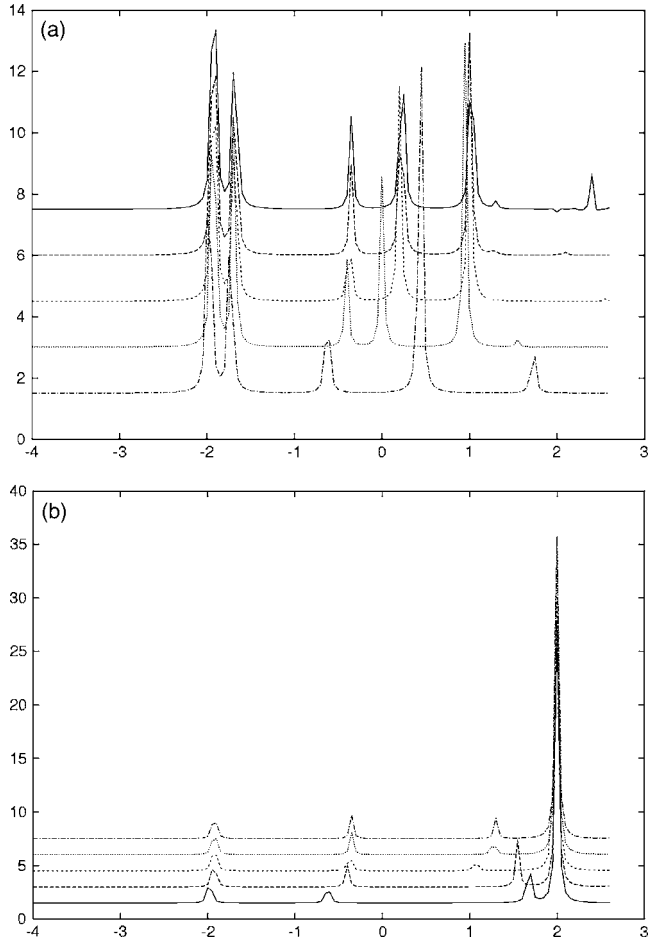

FIG. 5. The same as the previous Fig. but for $U=2$.

electronic states $|\uparrow,\downarrow\rangle$ and $|\uparrow\downarrow,0\rangle$ with a maximum of $N=5$ phonons are shown in Figs. 4–6 for different values of U and g.

VI. DISCUSSION

The recursive evaluation of the projected Green's function of Secs. V B and V C can be easily performed with an algebraic manipulation program. To demonstrate the qualitative tendencies the case for small numbers of phonons $N=1,2,3$ is discussed in the following. It should be noticed that much higher numbers can be studied with little effort. They show the same tendencies as those of small N.

A. Single-site model

In the strong-coupling regime the tunneling between the orbitals can be completely suppressed (i.e., $t=0$). Then the projected Green's function has only one pole, namely $z=0$. For any $t>0$, however, there are infinitely many poles due to the incomplete Gamma function in Eq. (11). But not all poles contribute with the same weight, as it is shown in Fig. 2. There are two effects: (i) Phonons lower the groundstate energy and (ii) the weight of the excitations decreases rapidly with increasing energy.

Eigenvalues in the weak-coupling regime in the absence of phonons (i.e., $N=0$, where $H_0=t\sigma_1+\omega_0 b^\dagger b\sigma_0$) are $E=\pm t$. This is a level splitting caused by the tunneling between the two orbitals. Already a single phonon lowers the ground state and creates new excited states, as shown in Fig. 3. Additional phonons do not affect the ground state but shift excited states and create new ones. In Fig. 3 this is plotted for phonon numbers up to $N=5$. The spectral weights of the excited states are also affected by the increasing number of phonons. All these effects are related to fact that the elements of the projected Green's function are rational functions

$$\frac{P_N(z)}{Q_N(z)}, \tag{16}$$

where N is the maximal number of phonons taken into account in the virtual processes. For $t=g=1$ and $N=0,1,2,3$ the Green's function $(\langle\uparrow|(z-H)^{-1}|\uparrow\rangle$ is calculated with MAPLE as

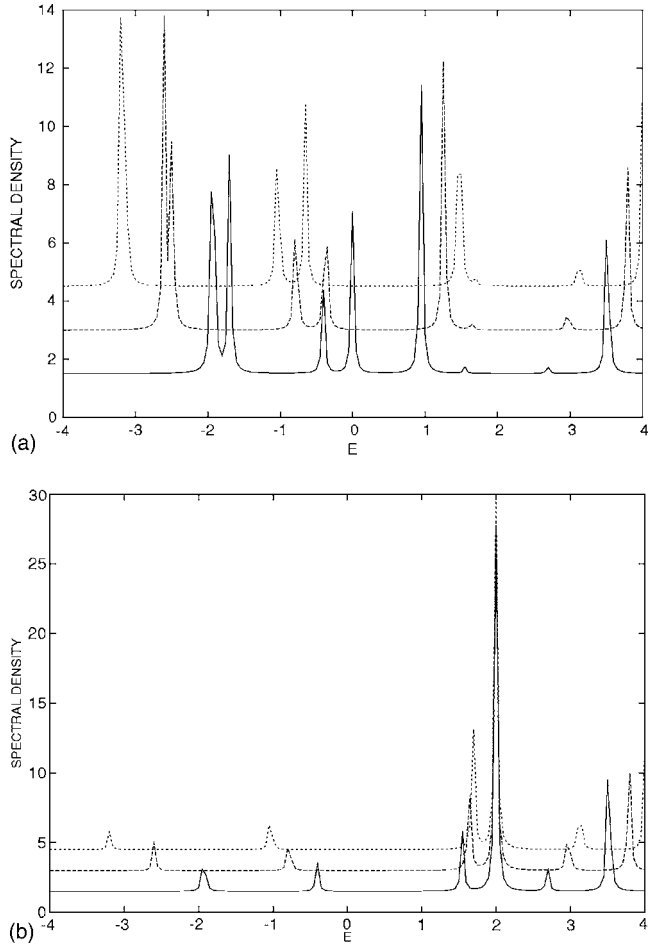

FIG. 6. The same as the previous Fig. but for $N=2$ and $g^2=1,2,3$. ($1.5g^2$ is added to the curves for better visibility.)

$N=0$:

$$\frac{z}{z^2-1}$$

$N=1$:

$$-\frac{-4z+z^3+7z^2+z^5-4z^4-1}{-5+4z^2+12z+z^4-14z^3+4z^5-z^6}$$

$N=2$:

$$-\frac{4+3z-46z^2+33z^4+24z^3+10z^6-33z^5-z^7}{-11-64z+46z^2+94z^3+31z^6-14z^5-82z^4-10z^7+z^8}$$

$N=3$:

$$-\frac{8-218z+701z^2-558z^3-449z^6+759z^5-361z^4+128z^7+z^9-18z^8}{-180+872z-716z^2-1156z^3-519z^6-440z^5+1809z^4+414z^7-z^{10}+18z^9-126z^8}.$$

Apparently, the order of the polynomial $P_N(z)$ is one less than the order of $Q_N(z)$ and increases by 2 for $N\geqslant 1$:

$$P_N(z)=z^{2(N+1)+1}+o(z^{2(N+1)}),\quad Q_N(z)=z^{2(N+2)}+o(z^{2(N+2)-1}).$$

B. Two-site model

In the case of two electrons on two sites there is tunneling between the two sites. Without phonons the Hamiltonian $H_0=H_e$ in Eq. (12) has eigenvalues

$$E=0,\ U,\ \frac{U\pm\sqrt{U^2+16t^2}}{2}.$$

Without Hubbard repulsion U there are three different eigenvalues, where the degeneracy of $E=0$ represents the states

$$E=0{:}|\uparrow,\downarrow\rangle+|\downarrow,\uparrow\rangle,\quad E=U{:}|\downarrow\uparrow,0\rangle+|0,\downarrow\uparrow\rangle.$$

With Hubbard repulsion $U>0$ there are four nondegenerate eigenvalues. The most obvious effect in this two-site model is the lowering of the ground state energy already by a single phonon and the creation of excitations on energies above the ground state energy. It is interesting to notice that more excitations contribute to the singly occupied Green's function $\langle\downarrow,\uparrow|(z-H)^{-1}|\downarrow,\uparrow\rangle$ than to the doubly occupied Green's function $\langle\downarrow\uparrow,0|(z-H)^{-1}|\downarrow\uparrow,0\rangle$. Moreover, there is always a state with maximal weight at $E=U$ for the state $|\downarrow\uparrow,0\rangle$.

The Green's function with maximally N phonons is again a rational function of the form (16). For $t=g=1$ and $U=0$ the expression

$$\langle\downarrow,\uparrow|(z-H)^{-1}|\downarrow,\uparrow\rangle=\frac{P_N(z)}{Q_N(z)}$$

is calculated with MAPLE as

$N=0$:

$$P_0(z)=z^2-2,\quad Q_0(z)=z(z^2-4)$$

$N=1$:

$$P_1(z)=(z^5-3z^4-7z^3+15z^2+8z-10)(z^2-2z-5)$$

$$Q_1(z)=z^8-5z^7-10z^6+62z^5+33z^4-221z^3-44z^2+176z-40$$

$N=2$:

$$P_2(z)=z^{10}-13z^9+49z^8+11z^7-378z^6+386z^5+720z^4-852z^3-536z^2+408z+144$$

$$Q_2(z)=z^{11}-13z^{10}+45z^9+61z^8-562z^7+396z^6+1788z^5-2092z^4-1368z^3+1632z^2+224z-192$$

$N=3$:

$$P_3(z)=z^{13}-24z^{12}+226z^{11}-1000z^{10}+1578z^9+3192z^8-15756z^7+15484z^6+16149z^5-35976z^4+8226z^3+15076z^2-7944z+672$$

$$Q_3(z)=z(z^{13}-24z^{12}+222z^{11}-906z^{10}+708z^9+7046z^8-22638z^7+9330z^6+61467z^5-98222z^4+18512z^3+56152z^2-38816z+7168).$$

Apparently, the order of the polynomial $P_N(z)$ is again one less than the order of $Q_N(z)$ and increases by 3 for $N\geqslant 1$:

$$P_N(z)=z^{3(N+1)+1}+o(z^{3(N+1)}),$$

$$Q_N(z)=z^{3(N+1)+2}+o(z^{3(N+1)+1}).$$

As shown in Figs. 4–6 the first three low-energy states are not affected if the phonon number exceeds $N=3$.

C. Physical interpretation

Experiments with molecules or small mesoscopic systems are usually dealing with single-electron effects.[20] This means that one could consider one electron at a single site that couples to the vibrational degress of freedom of the molecule. This site is contacted with leads such that an electron can enter or leave the molecular site through a tunneling process. The latter can be described by a phenomenological complex potential (or self energy).[20] In the case of a strong intramolecular interaction, however, a single-electron description is insufficient. Considering for instance the states of a two-site model given in Eq. (9), several scattering processes *inside* the molecular system can take place. In the case of the initial state $|\Psi_0\rangle=|\downarrow,\uparrow\rangle$ the simplest processes are

$$|\downarrow,\uparrow\rangle\rightarrow|\downarrow\uparrow,0\rangle\rightarrow|\downarrow,\uparrow\rangle,\quad|\downarrow,\uparrow\rangle\rightarrow|0,\downarrow\uparrow\rangle\rightarrow|\downarrow,\uparrow\rangle,$$

where phonons appear only in the intermediate state. If the initial state is $|\Psi_0\rangle=|\downarrow\uparrow,0\rangle$ the simplest processes are

$$|\downarrow\uparrow,0\rangle\rightarrow|\uparrow,\downarrow\rangle\rightarrow|\downarrow\uparrow,0\rangle,\quad|\downarrow\uparrow,0\rangle\rightarrow|\downarrow,\uparrow\rangle\rightarrow|\downarrow\uparrow,0\rangle,$$

where again phonons appear only in the intermediate state. These processes have very different properties (cf. Figs. 4–6). The large weight of $Im(\langle\downarrow\uparrow,0|(z-H)^{-1}|\downarrow\uparrow,0\rangle$ (lower panels) at $E=U$ has an interpretation by using the relation between the peak height h_ϵ and the overlap $|\langle E_j|\Psi_0\rangle|$ of Sec. II:

$$h_\epsilon\approx|\langle E_j|\Psi_0\rangle|^2/\epsilon.$$

Thus the results of Figs. 4–6 indicate that there is a large overlap for the eigenstate with energy U and the doubly occupied state $|\downarrow\uparrow,0\rangle$. On the other hand, the overlap of the eigenstates with $|\downarrow,\uparrow\rangle$ (upper panels in Figs. 4–6 is weak in comparison. This provides an experimental access to the strength of the intramolecular Coulomb interaction by measuring the spectral density of a molecular system.

The elements of the spectral function $Im\langle\Psi_0|(E-i\epsilon-H)^{-1}|\Psi_0\rangle$ usually can be measured only indirectly, for instance, by attaching leads to the molecule and measuring the current through the molecule.[2,3,21,22] In a strongly interacting electronic system this current is given as[20,23]

$$I = I_0 \epsilon \int \sum_j \frac{|\langle E_j|\Psi_0\rangle|^2}{(E-E_j)^2+\epsilon^2}[f_1(E)-f_2(E)]dE$$

$$\sim I_0 \sum_j |\langle E_j|\Psi_0\rangle|^2 [f_1(E_j)-f_2(E_j)] \quad (\epsilon \sim 0), \qquad (17)$$

where ϵ and the prefactor I_0 depend on the details of the leads and their coupling to the molecule. $f_1(E)$ and $f_1(E)$ are the Fermi function with respect to the two contacts and their chemical potentials μ_j at temperature T:

$$f_\nu(E) = (1 + e^{(E-\mu_\nu)/k_B T})^{-1}.$$

From the expression of the current in Eq. (17) the steps of the conduction at the poles E_j can easily be calculated.

VII. CONCLUSIONS

A a recursive method has been developed to study the spectral properties of small Jahn-Teller systems. It is based on a decomposition of the infinite-dimensional Hilbert space, spanned by a few electronic and an unlimited number of phononic states. Two cases were considered, one for an infinite number of phonons (the strong-coupling case) and one in which the number of phonons is increased by one in each iteration step of a recursive equation (the weak-coupling case). In both cases the iteration of the recursion relation leads to a continued-fraction representation of a projected Green's function. The matrix elements of the resulting Green's function are related to the incomplete Gamma function in the strong-coupling case and to rational functions in the weak-coupling case, respectively.

An advantage of this method is that it approaches the exact solution systematically by standard functions. It is an alternative to perturbative approaches, based on a power series of a model parameter (e.g., the tunneling rate t or the electron-phonon coupling constant g).

ACKNOWLEDGMENTS

I would like to thank K.-H. Höck and K. Becker for useful discussions. This work was supported by the Deutsche Forschungsgemeinschaft through Sonderforschungsbereich 484.

*Electronic address: Klaus.Ziegler@Physik.Uni-Augsburg.de

[1] N. C. van der Vaart, S. F. Godijn, Y. V. Nazarov, C. J. P. M. Harmans, J. E. Mooij, L. W. Molenkamp, and C. T. Foxon, Phys. Rev. Lett. **74**, 4702 (1995).
[2] J. R. Hahn and W. Ho, Phys. Rev. Lett. **87**, 196102 (2001).
[3] N. B. Zhitenev, H. Meng, and Z. Bao, Phys. Rev. Lett. **88**, 226801 (2002).
[4] W. G. van der Wiel, Rev. Mod. Phys. **75**, 1 (2003).
[5] M. V. Mostovoy and D. I. Khomskii, Phys. Rev. Lett. **89**, 227203 (2002).
[6] R. F. Bishop and C. Emery, J. Phys. A **34**, 5635 (2001).
[7] J. Ranninger and U. Thibblin, Phys. Rev. B **45**, 7730 (1992).
[8] A. S. Alexandrov, V. V. Kabanov, and D. K. Ray, Phys. Rev. B **49**, 9915 (1994).
[9] A. Weiße, G. Wellein, and H. Fehske, *High Performance Computing in Science and Engineering 2001*, edited by E. Krause and W. Jaeger (Springer, Heidelberg, 2002), p. 131.
[10] E. Berger, P. Valesek, and W. Linden, Phys. Rev. B **52**, 4806 (1995).
[11] S. El Shawish, J. Bonca, L. C. Ku, and S. A. Trugman, Phys. Rev. B **67**, 014301 (2003).
[12] P. Fulde, *Electron Correlations in Molecules and Solids* (Springer, Berlin, 1993).
[13] K. Ziegler, Phys. Rev. A **68**, 053602 (2003).
[14] I. I. Rabi, Phys. Rev. **51**, 652 (1937).
[15] S. Pairault, D. Sénéchal, and A.-M. S. Tremblay, Phys. Rev. Lett. **80**, 5389 (1998).
[16] M. Abramowitz and I. A. Stegun, *Handbook of Mathematical Functions* (Dover, New York, 1965).
[17] A. Macridin, G. A. Sawatzky, and M. Jarrell, Phys. Rev. B **69**, 245111 (2004).
[18] S. Swain, J. Phys. A **6**, 192 (1973).
[19] M. Capone and S. Ciuchi, Phys. Rev. B **65**, 104409 (2002).
[20] S. Datta, *Electronic Transport in Mesoscopic Systems* (Cambridge University Press, New York, 1995).
[21] B. C. Stipe, M. A. Rezaei, and W. Ho, Science **280**, 1732 (1998).
[22] J. R. Hahn and W. Ho, Phys. Rev. Lett. **87**, 166102 (2001).
[23] Y. Meir and N. S. Wingreen, Phys. Rev. Lett. **68**, 2512 (1992).